Upper critical magnetic field and vortex-free state in very thin epitaxial δ-MoN films grown by polymer-assisted deposition

2013 Supercond. Sci. Technol. 26 105023

(http://iopscience.iop.org/0953-2048/26/10/105023)

Supercond. Sci. Technol. **26** (2013) 105023 (7pp) doi:10.1088/0953-2048/26/10/105023

Upper critical magnetic field and vortex-free state in very thin epitaxial δ-MoN films grown by polymer-assisted deposition

N Haberkorn[1], Y Y Zhang[2], Jeehoon Kim[3], Thomas M McCleskey, Anthony K Burrell[4], R F Depaula, T Tajima, Q X Jia and L Civale

Los Alamos National Laboratory, Los Alamos, NM 87545, USA

E-mail: nhaberk@cab.cnea.gov.ar

Received 25 July 2013
Published 12 September 2013
Online at stacks.iop.org/SUST/26/105023

Abstract

We measured the thickness dependence of the superconducting properties in epitaxial δ-MoN thin films grown on α-Al_2O_3(001) substrates by polymer-assisted deposition. Our results indicate that the superconducting properties such as the upper critical field ($\mu_0 H_{c2} \approx 10$ T) and the superconducting critical temperature ($T_c = 12.5$ K) are thickness independent for films thicker than ∼36 nm. By measuring the critical current density (J_c) in the vortex-free state, which coincides with the depairing current density (J_0), we estimate that films thicker than ∼36 nm have a coherence length $\xi(0) = 5.8 \pm 0.2$ nm and penetration depth $\lambda(0) = 420 \pm 50$ nm. We found that it is possible to enhance the $H_{c2}(0)$ values to close to 10 T without any appreciable reduction in T_c.

(Some figures may appear in colour only in the online journal)

1. Introduction

Transition-metal carbides and nitrides are known for possessing high melting points and hardness [1] and, in some cases, attractive superconducting properties [2]. The molybdenum nitrides possess several crystalline phases: γ-Mo_2N (cubic) with a superconducting transition temperature $T_c \sim 5$ K [3], β-Mo_2N (tetragonal) with $T_c \sim 5$ K [4], and δ-MoN (hexagonal) with $T_c \sim 12$ K [5, 6]. Thin films and coatings are widely used to reduce friction and to protect bulk materials from abrasion, corrosion, oxidation, and thermal shock [7, 8]; and, from an electronic point of view, these materials have potential applications to device development [9–11]. Molybdenum nitride thin films have been grown by several techniques, such as reactive sputtering [12], pulsed laser deposition (PLD) [13], or by reacting a metallic Mo film with ammonia [14]. Christen *et al* [14] showed that cleaner δ-MoN film formed by the reaction of pure Mo film and NH_3 at 1873 K has $T_c \sim 13$ K and upper critical magnetic field $\mu_0 H_{c2}(0) \sim 4$–5 T.

It is known that H_{c2} can be enhanced, making the material more attractive for applications, by adding non-magnetic impurities [15, 16] that reduce the electronic mean free path (l). When l is smaller than the BCS (intrinsic) superconducting coherence length (ξ_0), the material is in the dirty limit and the effective coherence length (ξ) decreases and H_{c2} increases. Recently, we have reported high-quality epitaxial δ-MoN films grown by chemical solution deposition [17]. These films show $T_c \sim 13$ K and $\mu_0 H_{c2}(0) \sim 9$–10 T, which are similar to the values found for nitrogen ion (N)-irradiated films [14]. Potential technological applications of superconducting thin

[1] Present address: Centro Atómico Bariloche, Avenida Bustillo 9500 (8400) Bariloche, Argentina.

[2] Present address: Center for Nano and Micro Mechanics, Tsinghua University, Beijing 100084, People's Republic of China.

[3] Present address: Center for Artificial Low Dimensional Electronic Systems, Institute for Basic Science and Department of Physics, POSTECH, Pohang, 790-784, Korea.

[4] Present address: Chemical Sciences and Engineering Division, Argonne National Laboratory, 9700 S. Cass Avenue, Lemont, IL 60439, USA.

films usually demand targeted film properties. For example, single-photon detectors demand superconductors with short mean free path [18], whereas superconducting ratio frequency (SRF) cavities require films with thickness (d) $\ll$ penetration depth (λ) [11] in the clean limit [19].

The superconducting properties of thin films differ from those of the bulk when the thickness (d) is comparable to or smaller than either one of the two fundamental length scales, the coherence length (ξ) or the penetration depth (λ) [20–23]. This limit exhibits interesting physics and provides unique possibilities to determine superconducting parameters that are difficult to measure otherwise, such as the depairing current density (J_0), as discussed below. It is known that H_{c2} is higher when the magnetic field (**H**) is applied parallel to the surface ($H_{c2}^{\parallel S}$) in the so-called vortex-free state (when the film is too thin to nucleate a vortex core) as compared to the value when the field is normal to the surface ($H_{c2}^{\parallel c}$) [21, 24, 25]. According to phenomenological and microscopic theories [25], the critical field should vary with temperature (T) as $H_c^{\parallel S}(T) \propto (1-t)^{1/2}$, where $t = T/T_c$, independent of the ratio of ξ/l.

In this work we analyze the thickness dependence of the superconducting parameters $H_{c2}(T)$ and T_c of δ-MoN thin films grown by polymer-assisted deposition (PAD) [26], where the film thickness is in the range of technological significance for both electronic and mechanical applications. One of the main advantages of PAD is the ability to grow very thin films with homogeneous properties over large surface areas. Our results indicate that the PAD MoN films are in the dirty limit, and the properties are thickness independent for films thicker than ~36 nm, with $T_c \sim 12.6$ K. For **H** parallel to the surface we identify the vortex-free state in films of various thicknesses. In a 40 nm film with $\xi(0) = 5.8 \pm 0.2$ nm ($H_{c2} \sim$ 9–10 T), we take advantage of the vortex-free state to estimate J_0, λ, and the thermodynamic critical magnetic field (H_c).

2. Experimental details

Thin films with different thicknesses (d) of 18 (d18), 28 (d28), 36 (d36), 40 (d40) and 60 (d60) nm were grown on (001)-oriented α-Al_2O_3. Briefly, epitaxial δ-MoN films were grown on c-cut sapphire (Al_2O_3) substrates by a chemical solution deposition or PAD. The Mo precursor solution used in this work was prepared by dissolving 2.6 g of $(NH_4)_6Mo_7O_{24}{\cdot}4H_2O$ in 15.0 ml of H_2O, then mixing with 4.0 g of ethylenediaminetetraacetic acid (EDTA) and 3.5 g of polyethyleneimine (PEI) followed by ultrafiltration. The precursor solution was spin-coated on a c-cut sapphire substrate. The film thickness can be tuned by varying the spin speed and the number of coatings. The precursor films were annealed at 890 °C for 2 h in flowing NH_3 gas at an ambient pressure to obtain superconducting δ-MoN films [17]. The epitaxial growth of hexagonal δ-MoN on α-Al_2O_3 has been confirmed by x-ray diffraction (XRD), cross-sectional transmission electron microscopy (TEM) and high-resolution TEM (HRTEM) analysis. The films are oriented with the c-axis perpendicular to the substrate surface. The results obtained by different techniques are consistent, indicating that

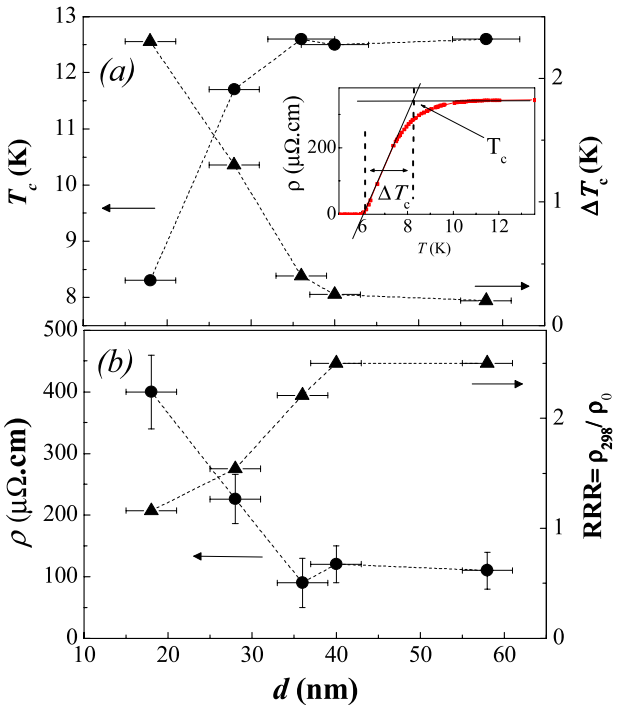

Figure 1. (a) Thickness dependence of the superconducting critical temperature (T_c) and the transition width (ΔT_c). Inset shows the criteria used to determine the T_c and ΔT_c. (b) Thickness dependence of the room temperature resistivity (ρ) and residual-resistivity ratio RRR $= \rho^{298}/\rho^0$.

epitaxial relationships between δ-MoN and the Al_2O_3 are $(0001)_{MoN} \parallel (0001)_{Al_2O_3}$ and $(10\bar{1}0)_{MoN} \parallel (11\bar{2}0)_{Al_2O_3}$. The root-mean-square (rms) surface roughness obtained by atomic force microscopy (AFM) for a 40 nm thick film, measured from a 4 μm × 4 μm area, is 3.8 nm. The thickness of the films was determined by x-ray reflectivity (XRR) measurements.

Electrical resistance measurements at different temperatures (T) and magnetic fields up 9 T were performed in a commercial Quantum Design PPMS system using the conventional four-probe method. The H_{c2} curves with **H** applied parallel ($H_{c2}^{\parallel S}$) and perpendicular ($H_{c2}^{\parallel c}$) to the surface were derived from the criteria shown in the inset of figure 1(a). The electrical transport measurements were performed on 1 mm (length) × 0.2 mm (width) bridges. A standard four-terminal transport technique was used to measure I–V curves. Critical current densities (J_c) were determined using a 1 μV cm^{-1} criterion. The spatial homogeneity of the superconductivity in d40 was analyzed by using an in-house-built low-temperature magnetic force microscope (MFM) apparatus [27]. We performed measurements of the Meissner response as a function of the tip–sample separation at different positions.

3. Results and discussion

Figure 1(a) shows the thickness dependence of T_c and the transition width (ΔT_c) of the δ-MoN films. The results show that $T_c \sim 12.5$ K and $\Delta T_c \sim 0.2$–0.3 K were maintained when $d \geq 36$ nm. Figure 1(b) shows the thickness dependence of the room-temperature ($T = 298$ K) resistivity (ρ_{298}) and the residual-resistivity ratio (RRR) (ρ_{298}/ρ_0). The ρ_0 values

(obtained by extrapolation to $T = 0$ from the normal state) are ~90 $\mu\Omega$ cm when $d \geq 36$ nm. The ρ_0 versus T_c dependence was previously discussed in [14]; we found ρ_0 values higher than those for nitrogen ion (N)-irradiated samples ($\rho_0 \sim 5\ \mu\Omega$ cm) with the same T_c. However, as we will discuss later, in our case and in particular for very thin films, the resistivity can be overestimated in films with inhomogeneities.

Figures 2(a) and (b) show $H_{c2}(T)$ for $d18$ and $d40$ with the magnetic field parallel ($H_{c2}^{\|S}$) and perpendicular ($H_{c2}^{\|c}$) to the surface. For the parallel field case, the $d18$ film shows the dependence $H_c^{\|S}(T) \propto (1-t)^{1/2}$, expected for vortex-free 2D behavior, in the whole range of temperature analyzed [28]. The films $d40$, $d36$ (not shown) and $d60$ (not shown) exhibit a similar behavior in $H_{c2}^{\|S}(T)$, with a nonlinear dependence close to T_c. In contrast to $d18$, however, these thicker samples show a change to linear dependence at lower temperatures. The crossover temperature depends on the thickness, in agreement with the expected 2D–3D crossover that appears when the ratio $d/\xi(T) = 4.4$ [29]. The observation of this vortex-free regime is one of the main results of this study. In the thinnest film ($d18$) the $H_{c2}^{\|c}(T)$ dependence shows a small shoulder close to T_c, a feature that is absent in all the thicker films where $H_{c2}^{\|c}(T)$ vanishes linearly at T_c. This feature may be due to inhomogeneity of the films; the percolation of the superconductivity in the thinnest film may occur through paths whose widths are in the range of $\xi(T)$ close to T_c, thus showing a vortex-free, 2D-like behavior in a narrow temperature range.

The $H_{c2}^{\|c}$ values for all the films are higher than previously reported on cleaner films, indicating that our samples are in the dirty limit ($\xi_0 > l$). Cleaner δ-MoN thin films show $H_{c2}(0) \sim 4$–5 T, and these values can be enhanced by irradiation with nitrogen ions to values above 10 T with a gradual drop in T_c [14]. Our films show a similar enhancement, but without reduction in T_c (for $d \geq 36$ nm). As was discussed in [14], the Werthamer, Helfand, and Hohenberg (WHH) model that corresponds to the dirty limit [30], $H_{c2}(0) = -0.69\delta H_{c2}/\partial T|_{T_c}$, only matches experiment close to T_c, and cannot describe the low temperature data, so we cannot use such model to calculate $H_{c2}^{\|c}(0)$. Using the simpler approach of extrapolating the $H_{c2}^{\|c}(T)$ data in figures 2(a) and (b), we estimate that $H_{c2}^{\|c}(0) \sim 10.5 \pm 0.5$ T ($d18$) and $H_{c2}^{\|c}(0) \sim 9.5 \pm 0.5$ T ($d40$), which using $\xi(0) = \sqrt{\Phi_0/(2\pi H_{c2}^{\|c}(0))}$ corresponds to $\xi(0) = 5.5 \pm 0.2$ nm and $\xi(0) = 5.8 \pm 0.2$ nm, respectively. Very similar values to $d40$ are obtained for $d36$ and $d60$. This $\xi(0)$ value is higher than those previously reported in the cleaner films $\xi_0 \approx 9$ nm [14]. In an impure superconductor $\xi(0) = (\xi_0 l)^{1/2}$, although the data previously published in [14] do not correspond necessarily to the clean superconducting limit, $\xi_0 \approx 9$ nm sets an upper limit $l < 3.7$ nm in our films. The $H_{c2}^{\|c}(T)$ dependence for $d18$ suggests a value higher than 10 T. However, as we discussed before, this sample may have inhomogeneous microstructures, and the $H_{c2}^{\|c}(0)$ can be affected by dimensional effects.

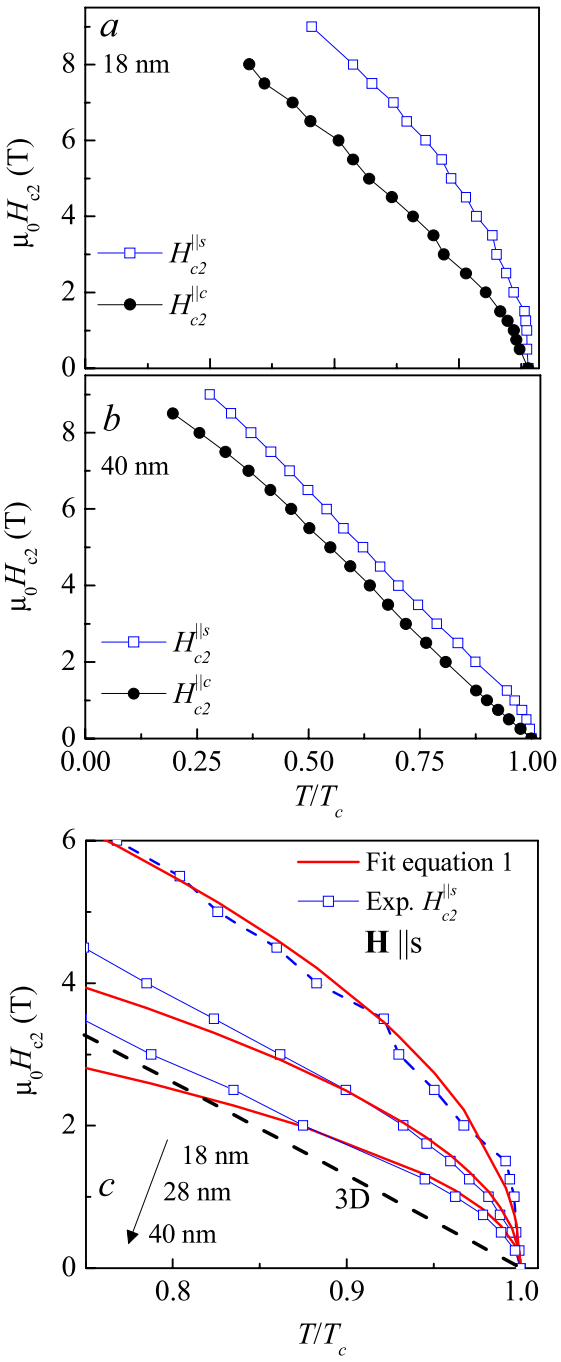

Figure 2. (a) and (b) Temperature dependence of the upper critical field (H_{c2}) with **H** parallel and perpendicular to the surface for samples $d18$ and $d40$, respectively. (c) Temperature dependence of the upper critical field (H_{c2}) with **H** parallel to the surface for three different films. Fits using equation (1) are also shown. Dashed line (3D) corresponds to the $H_c^{\|c}(T)$.

Figure 2(c) shows the $H_{c2}^{\|S}(T)$ dependence close to T_c for $d18$, $d28$ and $d40$. In the dirty limit $H_{c2}^{\|S}(T)$ is given by [31]

$$H_{c2}^{\|S}(T) = \frac{\sqrt{3}\Phi_0}{\pi d\xi(T)} = \frac{\sqrt{3}\Phi_0}{\pi d\left[0.855(\xi_0 l)^{1/2}\right]}(1-t)^{1/2} \quad (1)$$

where $\Phi_0 = 2.07 \times 10^{-7}$ G cm^2 is the flux quantum, The second equality arises from the Ginzburg–Landau (GL)

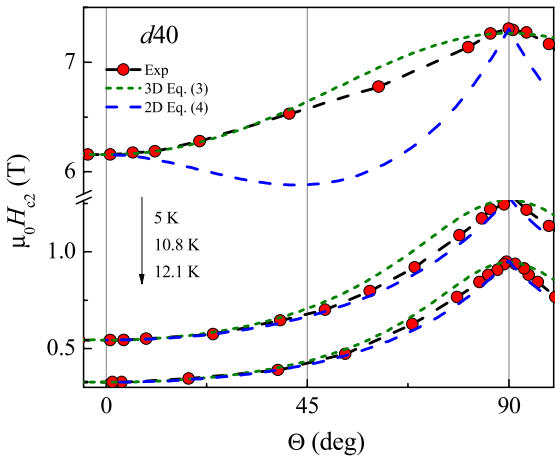

Figure 3. Angular dependence of the upper critical field (H_{c2}) at different temperatures in a MoN thin film with $d = 40$ nm.

relation in the dirty limit

$$\xi(T) = 0.855\xi(0)(1-t)^{-1/2}. \quad (2)$$

Although the principle of GL temperature dependences is only valid near T_c as pointed out by Tinkham, this approximation is accurate over a much wider temperature range because the local approximation remains until $T < T_c$. We use equation (2) to fit $H_{c2}^{\|c}(T)$ in the limit $T \to T_c$ with $\xi(0) = 5.8 \pm 0.2$ nm for both $d18$ and $d40$. The fits by using equation (1) for $H_{c2}^{\|S}(T)$ are shown in figure 2(c). We obtain good agreements by using a film thickness of 17 nm, 25 nm and 36 nm for samples $d18$, $d28$ and $d40$, respectively. This is in agreement with the surface roughness obtained by AFM. Also the fits are in agreement with the experimental data in the whole temperature range ($t > 0.8$) for $d18$, but only for a limited range close to T_c for the thicker films, confirming the presence of a vortex-free state in these films, which are in the dirty limit.

Figure 3 shows $H_{c2}(\Theta)$ for $d40$. For an infinite anisotropic superconductor, the dependence $H_{c2}(\Theta)$ on the field angle is a smooth curve over the entire Θ range, with no cusp-like behavior at $\Theta = 90°$, which is well reproduced within the anisotropic effective mass GL theory:

$$H_{c2}(\Theta) = H_{c2}(\Theta = 0)(\cos^2\Theta + \gamma^{-2}\sin^2\Theta)^{-1/2}, \quad (3)$$

where $\gamma = H_{c2}^{\|S}/H_{c2}^{\|c}$ is the anisotropy parameter. In contrast, for very thin superconducting films in the 2D limit $\xi(T) \gg d$ with two flat surfaces, Tinkham derived the formula for the critical field $H_c(\Theta)$ dependence [21]

$$\left|\frac{H_c(\Theta)\sin\Theta}{H_c(\pi/2)}\right| + \left|\frac{H_c(\Theta)\cos\Theta}{H_c(0)}\right|^2 = 1, \quad (4)$$

which gives a discontinuous derivative $dH_{c2}/d\Theta$ at $\Theta = 90°$. As discussed by Tinkham [25], in the temperature regions where our films are in the 2D limit we can identify H_c with our H_{c2}.

The results show that close to T_c the $H_{c2}(\Theta)$ for $d40$ can be scaled using equation (4), which is also evident from the cusp-like feature around 90°. However, at low temperatures the results can be scaled using neither equation (3) nor (4). Yuan *et al* [28] demonstrated that the 2D–3D crossover can happen in films of intermediate thickness, when $d/2\xi > 1.7$, and the angular dependence of H_{c2} can deviate significantly from that of equation (3). We also found that the angular dependence in $d60$ (not shown) cannot be scaled by either equations (3) or (4), which suggests that the small anisotropy observed at low temperatures ($\gamma = H_{c2}^{\|S}/H_{c2}^{\|c} \sim 1.15$) may be associated with dimensional effects and not with the effective mass anisotropy.

The highest possible non-dissipative current density in a superconductor is the depairing current density (J_0) that corresponds to the kinetic energy associated with the supercurrents when they exceed the binding energy of the Cooper pairs. The experimental critical current density (J_c) in bulk type II superconductors and superconductor films, on the other hand, is determined by the dissipation associated with vortex motion, and is typically one or more orders of magnitude lower than J_0. However, in the case of very thin films or wires (i.e., the vortex-free state) [25], the experimental J_c should be the maximum possible critical current density limited by depairing [32, 33]. For conventional superconductors the temperature dependence of J_0 near T_c is given by the GL expression

$$J_0^{GL}(t) = \frac{cH_c(T)}{3\sqrt{6}\pi\lambda(T)} \propto J_0^{GL}(0)(1-t)^{3/2}, \quad (5)$$

where $H_c(0) = \frac{\Phi_0}{2\sqrt{2}\pi\lambda(0)\xi(0)}$ is the thermodynamic critical field, $H_c(t) = 1.73H_c(0)(1-t)$, $\lambda_L(t) = \frac{\lambda_L(0)}{[2(1-t)]^{1/2}}$ and $\lambda(t)|_{\text{dirty limit}} = \lambda_L(t)(\frac{\xi_0}{1.33l})^{1/2}$, and $J_0^{GL}(0)$ is the depairing current density at zero temperature, c is the speed of light in vacuum, and H_c is the thermodynamic critical field. Figure 4(a) shows $[0.26J_0(t)/J_0(0)]^{2/3}$ versus T/T_c for $d40$ with $H \parallel S$ (0.05 T); the magnetic field was applied in order to avoid the presence of vortices by decreasing the transverse magnetic field component from self-field effects. The *constant* 0.26 appears by considering the equivalence in equation (5), and the $H_c(t)$ and $\lambda(t)$ dependence. Figure 4(b) shows $J_c(\Theta)$ at 11 K; the results show the typical angular dependence expected from vortex pinning by randomly distributed point defects [34]. The inset in figure 4(b) shows that the alignment between the films and **H** used to derive the values shown in figure 4(a) is better than 0.05°. Using equation (5) and the relation $H_c = \frac{\Phi_0}{2\sqrt{2}\pi\lambda(0)\xi(0)}$ and the data plotted in figure 4(a), we estimate $J_0^{GL}(0) \sim 9$ mA cm^{-2}, where we have used the previously estimated values of $\xi(0) = 5.8 \pm 0.2$ nm, $\lambda(0) = 440 \pm 40$ nm, and $H_c(0) = 900 \pm 100$ Oe. Our value for the depairing currents is around 5 times smaller than that reported for a polycrystalline δ-MoN thin film [35]. This is consistent with the large $\lambda(0)$ in our films (see equation (5)). Figure 4(c) shows $J_c(H)$ with $H \parallel S$ and $H \parallel c$ at 10.5 and 11.25 K. The data show that in both configurations the J_c values are similar for $H \to 0$, which indicates the presence of few vortices at $\mu_o H = 0$. When the magnetic field is increased with $\mathbf{H} \parallel c$, then J_c drops fast as a consequence of vortex dissipation.

In order to verify the homogeneity of the superconductivity in our system, we measured the Meissner response force

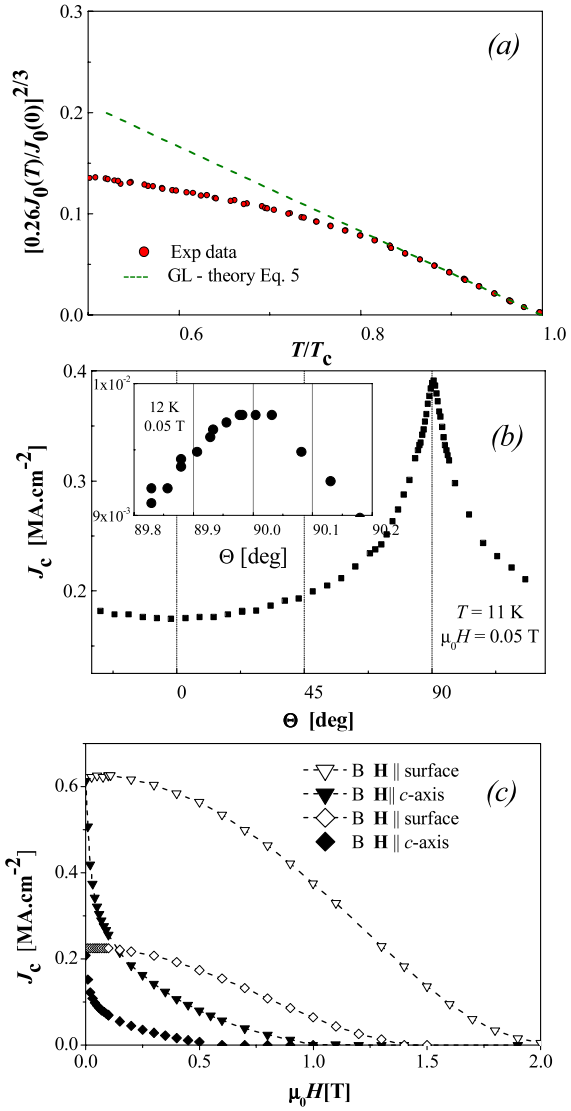

Figure 4. (a) Normalized depairing current versus temperature. The dotted line corresponds to the GL theory using equation (5). (b) Angular dependence of the critical currents at 11 K and 0.05 T. The inset corresponds to the alignment with the magnetic field (**H**) parallel to the surface (90°) at 12 K. (c) Critical current density versus magnetic field (**H**) parallel and perpendicular to the surface at 10.5 and 11.5 K.

between the probe tip and the sample using an MFM on the same film as analyzed in figure 4 [36]. Figure 5 shows a summary of the results. The Meissner signal corresponds to the partial screening ($\lambda \gg d$) and is sensitive to the value of λ. The analysis in three different places shows exactly the same Meissner response (and thus λ) within the experimental error, which indicates that there are no macroscopic dead superconductor regions such as islands or local suppression of superconductivity which can affect our measurement results.

To analyze more carefully the J_0 values obtained in the vortex-free state of our reference film, we performed J_0 versus H with $H \parallel S$ measurements on the film $d40$. According to the GL theory, depending on the ratio λ/d the parallel critical field ($H_c^{\parallel s}$) exceeds H_c by a large factor [25], $H_c^{\parallel s} = 2\sqrt{6}\frac{H_c\lambda}{d}$ and the expected J_0 versus H dependence is given by

$$J_0(H) = J_0(H = 0)(1 - (H/H_c^{\parallel s})^2). \quad (6)$$

Figure 6 shows $J_0/J_0(H = 0)$ versus $H/H_c^{\parallel s}$ at different temperatures (where $H_c^{\parallel s}(T)$ was obtained from the data in figure 2) and the fit using equation (6). The same scaling for all the curves indicates that the film is in the vortex-free state at all the temperatures in the range interested. At low magnetic fields we found the experimental data to be in good agreement with equation (6). The inset in figure 6 shows the good agreement between $H_c^{\parallel s}(T)$ obtained experimentally and the estimated value by considering $H_c(T)$ and $\lambda(t)|_{\text{dirty limit}}$ estimated by considering $d = 40$ nm. However, at high fields the superconductivity remains 20–25% above the $H_c^{\parallel s}$ values obtained in the fit. Assuming homogeneous superconducting parameters such as λ and ξ (this is reasonable considering the MFM results, the small ΔT_c and the coincidence of the $H_{c2}^{\parallel c}$ data for different films), the tail at large magnetic field is consistent with a local reduction of the effective film thickness (by ∼20–25%) due to the presence of surface roughness. This implies that the effective cross section of the film is smaller, which indicates that we may be underestimating $J_0^{GL}(0)$, but the difference must be significantly less than 25%, setting an upper limit for $J_{cd}^{GL}(0) \sim 11.2$ mA cm^{-2}, which corresponds to $\lambda(0) = 390 \pm 40$ nm and $H_c(0) = 1000 \pm 100$ Oe.

4. Conclusions

In conclusion, we have studied the superconducting properties of δ-MoN thin films grown by PAD. We found that the properties are thickness independent when $d \geq 36$ nm. Our measurements indicate that the films are in the dirty limit ($l < \xi_0$), and the H_{c2} values are consistent with those previously reported on irradiated films [14]. We found that the upper critical field anisotropy is dominated by dimensional effects, and the results suggest that the films should be isotropic in the 3D limit. All of the films analyzed are in the limit where $\lambda \gg d$; this limit is of technological relevance for SRF cavities [11]. We observed the vortex-free state over the whole temperature range in the thinnest film and above a 2D–3D crossover temperature in the thicker ones. We measured $J_0(H, T)$ in the vortex-free state, and by using the GL equations we estimated superconducting parameters, such as $\lambda(0)$ and $H_c(0)$ with values of 420 ± 50 nm and $H_c(0) = 950 \pm 150$ Oe, in the limit where the Meissner effect only provides partial screening. We did not observe the presence of dead regions in the superconducting films. The same $\lambda(0)$ and $H_c(0)$ values are expected in thicker films given the similarities of T_c, ΔT_c, and $H_{c2}(T)$ in these samples. Also, we found that it is possible to enhance the H_{c2} values to 10 T without appreciable decrease in T_c. Our approach provides a method to accurately measure $J_0(H, T)$, an important superconducting parameter both for fundamental understanding of vortex physics and technological applications.

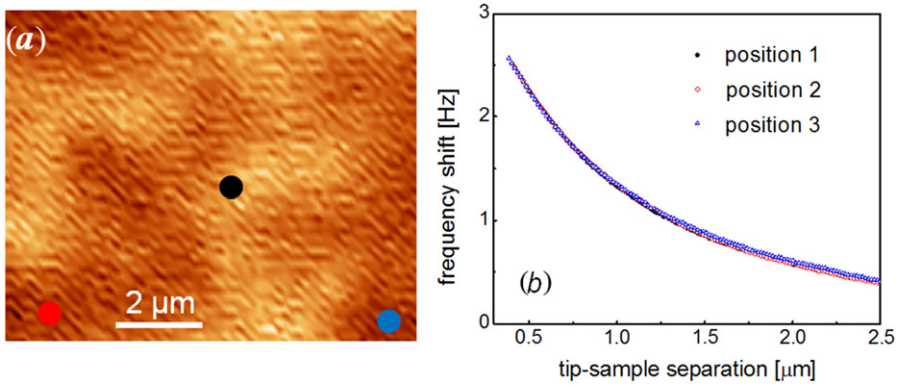

Figure 5. (a) Magnetic force microscopy (MFM) image of the film *d*40 taken at 4 K in the Meissner state. (b) Meissner response force as a function of tip–sample separation at 4 K in the regions indicated with solid circles in (a).

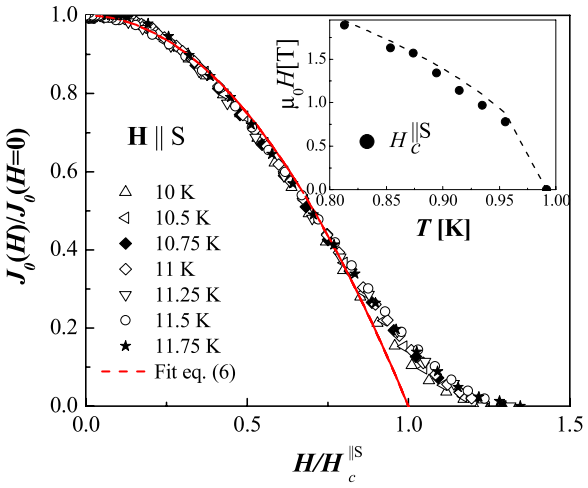

Figure 6. Normalized superconducting depairing current versus magnetic field (H) normalized by $H_c^{\|s}$ obtained from equation (6). The inset shows the reduced temperature (T/T_c) dependence of the $H_c^{\|s}$ values used in the normalization. The dashed line corresponds to the simulation by considering $H_c(t)$ and $\lambda(t)$.

Acknowledgments

Research was supported by the US Department of Energy, Office of Basic Energy Sciences, Division of Materials Sciences and Engineering (transport and MFM measurements, theoretical interpretation, data analysis and manuscript preparation), and by Tajima 2010 DOE Early Career Award (films fabrication). This work was also supported, in part, at the Center for Integrated Nanotechnologies (CINT), an Office of Science User Facility operated for the US Department of Energy Office of Science. Access to the PPMS system was granted through CINT user project no. U2009B059. NH is a member of CONICET (Argentina). We thank Cristian Batista and Shi-Zeng Lin for helpful discussions.

References

[1] Toth L E 1971 *Transition Metal Carbides and Nitrides* (New York: Academic)
Storms E K 1967 *The Refractory Carbides* (New York: Academic)
[2] Dew-Hughers D and Jones R 1980 *Appl. Phys. Lett.* **36** 856
[3] Matthias B T and Hulm J K 1952 *Phys. Rev.* **87** 799
[4] Inumaru K, Baba K and Yamanaka S 2005 *Chem. Mater.* **17** 5935
[5] Ettmayer P and Monatsch P 1970 *Monatsch Chem.* **101** 127
[6] Jehn H and Ettmayer P 1978 *J. Less-Common Met.* **58** 85
[7] Soignard E, MacMillan P F, Chaplin T D, Farag S M, Bull C L, Somayazulu M S and Leinenweber K 2003 *Phys. Rev.* B **68** 132101
[8] Bull C L, McMillan P F, Soignard E and Leinenweber K 2004 *J. Solid State Chem.* **177** 1488
[9] Palmieri V 2001 New materials for superconducting radiofrequency cavities *The 10th Workshop on RF Superconductivity (Tsukuba)* p 162
[10] Gol'tsman G N, Okunev O, Chulkova G, Lipatov A, Semenov A, Smirnov K, Voronov B, Dzardanov A, Williams C and Sobolewski R 2001 *Appl. Phys. Lett.* **79** 705
[11] Gurevich A 2006 *Appl. Phys. Lett.* **88** 012511
[12] Ihara H, Hirabayashi M, Senzaki K, Kimura Y and Kezuka H 1985 *Phys. Rev.* B **32** 1816
[13] Inumaru K, Baba K and Yamanaka S 2006 *Phys. Rev.* B **73** 52504
[14] Christen D K, Sekula S T, Ellis J T, Lewis J D and Williams J M 1987 *IEEE Trans. Magn.* **23** 1014
[15] Fietz W A and Webb W W 1967 *Phys. Rev.* **161** 423
[16] Gennes P G 1964 *Phys. Kondens. Mater.* **3** 79
[17] Zhang Y Y *et al* 2011 *J. Am. Chem. Soc.* **133** 20735
[18] Semenov A, Engel A, Il'in K, Gol'tsman G, Siegel M and Hübers H-W 2003 *Eur. Phys. J. Appl. Phys.* **21** 171
[19] Matricon J and Saint-James D 1967 *Phys. Lett.* A **24** 241
[20] Saint James D and de Gennes P G 1963 *Phys. Lett.* **7** 306
[21] Tinkham M 1963 *Phys. Rev.* **129** 2413
Tinkham M 1964 *Phys. Lett.* **9** 217
[22] Burger J P, Deutscher G, Guyon E and Martinet A 1965 *Phys. Rev.* **137** 853
[23] Bose S, Raychaudhuri P, Banerjee R, Vasa P and Ayyub P 2005 *Phys. Rev. Lett.* **95** 147003
[24] Bose S, Raychaudhuri P, Banerjee R and Ayyub P 2006 *Phys. Rev* B **74** 224502
[25] Tinkham M 2004 *Introduction to Superconductivity* 2nd edn (New York: Dover)
[26] Jia Q X, McCleskey T M, Burrell A K, Lin Y, Collis G E, Wang H, Li A D Q and Foltyn S R 2004 *Nature Mater.* **3** 529
[27] Nazaretski E, Graham K S, Thompson J D, Wright J A, Pelekhov D V, Hammel P C and Movshovich R 2009 *Rev. Sci. Instrum.* **80** 083704

[28] Yuan B J and Whitehead J P 1994 *Physica* C **231** 395
[29] Takezawa N, Koyama T and Tachiki M 1993 *Physica* C **207** 231
[30] Werthamer N R, Helfand E and Hohenberg P C 1966 *Phys. Rev.* **147** 295
[31] Abrikosov A A 1964 *Sov. Phys.—JETP* **20** 480
[32] Geers J M E, Hesselberth M B S, Aarts J and Golubov A A 2001 *Phys. Rev.* B **64** 94506
[33] Rusanov A Yu, Hesselberth M B S and Aarts J 2004 *Phys. Rev.* B **70** 24510
[34] Civale L *et al* 2004 *J. Low Temp. Phys.* **135** 87
[35] Karki A B, Young D P, Adams P W, Okudzeto E K and Chan J Y 2008 *Phys. Rev* B **77** 212503
[36] Luan L, Auslaender O M, Lippman T M, Hicks C W, Kalisky B, Chu J and Moler K A 2010 *Phys. Rev.* B **81** 100501(R)